

# Delamination Buckling and Postbuckling of Composite Cylindrical Shells

Haozhong Gu\* and Aditi Chattopadhyay†  
Arizona State University, Tempe, Arizona 85287-6106

A higher-order shear deformation theory is developed for accurately evaluating the transverse shear effects in delamination buckling and postbuckling of cylindrical shells under axial compression. The theory assures an accurate description of displacement field and the satisfaction of stress-free boundary conditions for the delamination problem. The governing differential equations of the present theory are obtained by applying the principle of virtual displacement. The Rayleigh-Ritz method is used to solve both linear and nonlinear equations by assuming a double trigonometric series for the displacements. Both linearized buckling analysis and nonlinear postbuckling analysis are performed for axially compressed cylindrical shells with clamped ends. Comparisons made with the classical laminate theory and a first-order theory show significant deviations.

## Nomenclature

$\mathbf{a}$	= generalized displacements
$B_{k^*}$	= differentiation operator, $k^* = 1, 2, \dots, 3(2N + 2)$
$E_L, E_T$	= elastic moduli of lamina in longitudinal and transverse directions, respectively
$G_{LT}, G_{TT}$	= shear moduli in the plane perpendicular and parallel to longitudinal direction of lamina, respectively
$H(h_1)$	= step function
$h$	= shell thickness
$K_L K_N$	= linear and nonlinear part of direct stiffness matrixes
$K_G$	= geometric stiffness matrix
$L$	= axial length of shell
$L_k$	= linear operator, $k = 1, 2, \dots, 3(2N + 1)$
$N$	= order used to evaluate transverse shear effect
$N_{ij}^{(k)}$	= defined stress resultants, $i, j = 1, 2, \dots, 6; k = 0, 1, 2$
$N_k$	= nonlinear operator, $k = 1, 2, \dots, 3(2N + 1)$
$p$	= in-plane compressive load distribution
$Q_{ij}$	= lamina stiffness components, $i, j = 1, 2, \dots, 6$
$R$	= radius of curvature of shell
$U_{\alpha j}^{(i)}, W^{(i)}$	= $j$ th order displacement functions, $\alpha = 1, 2; i = 0, 1, 2; j = 0, 1, \dots, N$
${}^0U_{\alpha j}^{(i)}, {}^0W^{(i)}$	= displacement components corresponding to the primary position
$u_i$	= displacement components, $i = 1, 2, 3$
$z^*$	= distance measured from shell midsurface to delamination interface
$\alpha$	= thickness parameter of delamination layer $2h_1/h$
$\beta L$	= delamination length
$\Gamma_\sigma$	= shell boundary in which compressive load is applied
$\Gamma_\Omega$	= boundary of whole shell
$\Gamma_{\Omega_d}$	= interfaces between delamination region and nondelamination region
$\varepsilon_i$	= strain components $i = 1, 2, \dots, 6$
$\eta_{k^*}$	= prescribed traction or displacement, $k^* = 1, 2, \dots, 3(2N + 2)$
$\lambda$	= eigenvalue

$\nu_{LT}, \nu_{TL}$	= Poisson's ratio in longitudinal and transverse directions, respectively
$\Pi$	= total potential energy
$\sigma_i$	= stress components, $i = 1, 2, \dots, 6$
$\sigma_{ij}^{(k)}$	= stress resultants $i = 1, 2, \dots, 6; j = 0, 1, \dots, N; k = 0, 1, 2$
$\psi_{im}$	= identified functions of displacements, $i = 0, 1, 2; m = N - 1, N$
$\Omega$	= region of whole shell
$\Omega_d$	= delamination region of shell

## I. Introduction

THE problem of delamination buckling and postbuckling of composite laminates has generated significant research interest and has been the subject of several theoretical investigations.<sup>1-5</sup> However, questions remain regarding a complete understanding and details of the phenomena involved. The problem of delamination buckling of cylindrical shells has not received adequate attention. Very few investigations have been reported in this area, especially in postbuckling analysis. Two separate studies were reported for solving the problem of buckling of layered cylindrical shells.<sup>6,7</sup> The effect of longitudinal delamination, assumed to extend over the entire length of the shell, in a laminar cylindrical shell subject to external pressure was examined by Troshin.<sup>8</sup> A more advanced model was presented for the study of delamination buckling of axially loaded cylindrical shells as well as delamination buckling and postbuckling of external pressure loaded cylindrical shells.<sup>9-11</sup> Kardomateas and Chung<sup>12</sup> introduced the thin-film model approximation for the problem of delamination buckling in external pressure loaded laminated cylindrical shells. In this work, the unbuckled portion of the shell was considered infinitely thick with respect to the delamination layer, and the first approximation scheme was used to derive the closed-form expressions of the critical pressure. With no exception, the analyses of multilayered cylindrical shells have been conducted only by using the classical laminate theory based on Kirchhoff hypothesis. It is well known that this theory is adequate for isotropic shells only when the thickness-to-radius ratio is very small. When fiber-reinforced composites are considered, the transverse shear strains must be taken into account since the ratio between the layer extentional modulus along the fiber direction and the shear modulus is usually very large.

Many efforts have been made in developing various two-dimensional shear deformable laminate theories,<sup>13</sup> and even three-dimensional layer-wise techniques,<sup>14</sup> to address the buckling problem of composite cylindrical shells without delamination. However, in the presence of delamination, the regular two-dimensional theories are no longer valid under the no contact assumption at delamination surface since in such a problem the transverse shear stresses ( $\tau_{xz}, \tau_{yz}$ ) must vanish not only at the surfaces but also at the

Received Feb. 24, 1995; revision received Feb. 10, 1996; accepted for publication Feb. 12, 1996. Copyright © 1996 by the American Institute of Aeronautics and Astronautics, Inc. All rights reserved.

\*Graduate Research Assistant, Department of Mechanical and Aerospace Engineering, Student Member AIAA.

†Associate Professor, Department of Mechanical and Aerospace Engineering, Senior Member AIAA.

delaminated interfaces. Therefore, a higher-order shear deformation theory (excluding the first-order theory) for addressing delamination modeling in composites cannot be a simple extension of the regular theory. Recently, Chattopadhyay and Gu<sup>15,16</sup> presented a new higher-order shear deformation theory to address delamination buckling of composite plates. By modification of the displacement field of regular higher-order theory,<sup>17</sup> an appropriate kinematic field, which can describe separation and slipping between the delaminated layer and the sublaminates, was proposed. Some higher-order shear correction terms were identified to ensure that the refined displacement field satisfies the transverse shear stress free boundary conditions at both plate surfaces and debonding interfaces. The results obtained using the new theory showed excellent agreement with available experimental data for composite plates. It was shown that the new theory provides an effective solution tool for accurate analysis of composite laminates with delaminations.

Composite laminated cylindrical shells are currently being used as a primary load-carrying structure in aerospace vehicles. To achieve the same strength as materials, in some applications, thicker walls are required that in turn reduce the ratio of the initial radius of curvature to total thickness. To efficiently analyze such structures in the presence of delamination, it is necessary to develop an accurate analysis procedure for delamination buckling and postbuckling of these thicker laminated shells. A generalized consistent theory is considered to provide better insight into the deformation and failure mechanism of these structures and is the subject of this research.

In this paper, the new higher-order theory, which was developed by Chattopadhyay and Gu<sup>15,16</sup> to characterize delamination successfully in laminated composite plates, is extended to model delamination buckling and postbuckling of cylindrical shells of perfect geometry subjected to the uniform axial load. The basic assumptions made in the theory are 1) no delamination growth during buckling and postbuckling, 2) the neglect of normal strains,  $\varepsilon_{zz} = 0$ , and 3) no contact at delaminated surfaces. This theory assures an accurate description of displacement field and the satisfaction of transverse shear traction-free boundary conditions for the delamination problem. The governing equations of the theory are derived by using the virtual displacement principle. Both linearized buckling analysis and postbuckling analysis are performed. Numerical results are presented and compared with existing solutions.

## II. Mathematical Formulation

### A. Higher-Order Theory for Delaminated Shells

For laminated circular cylindrical shells, the new higher-order theory is used to accurately describe the displacement components as follows:

$$u_\alpha = \sum_{j=0}^N z^j \{ U_{\alpha j}^{(0)} + [1 - H(z^*)] U_{\alpha j}^{(1)} + H(z^*) U_{\alpha j}^{(2)} \} \quad \alpha = 1, 2$$

$$u_3 = W^{(0)} + [1 - H(z^*)] W^{(1)} + H(z^*) W^{(2)} \quad (1)$$

where  $U_{\alpha 0}^{(0)}$  and  $W^{(0)}$  are the displacements at a point  $x_\alpha$  ( $\alpha = 1, 2$ ) on the midsurface,  $U_{\alpha j}^{(0)}$  ( $j = 1, 2, \dots, N$ ) are the  $j$ th-order transverse shear correction terms, and  $H(z^*)$  is the Heaviside step function described as

$$H(z^*) = H(z - z^*) = \begin{cases} 1 & z \geq z^* \\ 0 & z < z^* \end{cases} \quad (2)$$

where  $z^*$  represents the location of the delamination (Fig. 1). The jumps in displacement between the sublaminates and the buckling layer are given by  $U_{\alpha j}^{(1)}$ ,  $W^{(1)}$  and  $U_{\alpha j}^{(2)}$ ,  $W^{(2)}$  ( $\alpha = 1, 2$ ;  $j = 0, 1, \dots, N$ ), respectively. Note that the terms related to the delamination,  $U_{\alpha j}^{(k)}$ ,  $W^{(k)}$ ,  $k = 1, 2$ , exist only in the delamination region  $\Omega_d$ ; otherwise, they are zero. The use of the step function  $H(z^*)$  allows the kinematic description for separation and slipping as a result of the independence of the displacements, shown in Eq. (1), on adjacent layers at the delamination interface.

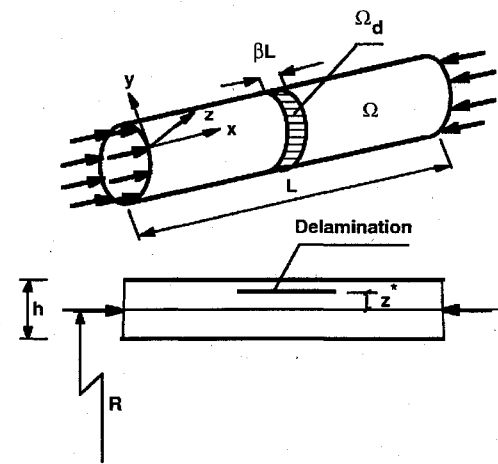


Fig. 1 Geometry of cylindrical shell with delamination.

In the buckling analysis, the nonlinear strains as a result of large radial displacements are taken into account. The following nonlinear Mushtari–Vlasov–Donnell strain-displacement relations<sup>14</sup> are used:

$$\varepsilon_1 = \varepsilon_{11} = u_{1,x} + \frac{1}{2} u_{3,x} u_{3,x}$$

$$\varepsilon_2 = \varepsilon_{22} = u_{2,y} + (u_3/R) + \frac{1}{2} u_{3,y} u_{3,y}$$

$$\varepsilon_4 = 2\varepsilon_{23} = u_{2,z} + u_{3,y} - (u_2/R) \quad (3)$$

$$\varepsilon_5 = 2\varepsilon_{13} = u_{1,z} + u_{3,x}$$

$$\varepsilon_6 = 2\varepsilon_{12} = u_{1,x} + u_{2,y} + u_{3,x} + u_{3,y}$$

The layer constitutive equation can be written as follows:

$$\sigma_i = Q_{ij} \varepsilon_j, \quad i, j = 1, 2, \dots, 6 \quad (4)$$

Note that the expression for displacement, as stated in Eq. (1), does not satisfy the transverse shear stress-free boundary conditions. These stress-free boundary conditions in delamination problems require that the transverse shear stresses  $\sigma_4$  and  $\sigma_5$  vanish on the shell inner and outer surfaces and on the debonding surfaces in delamination region. That is,

$$\sigma_4(x, y, \pm h/2) = 0 \quad (x, y) \in \Omega$$

$$\sigma_5(x, y, \pm h/2) = 0$$

$$\sigma_4^\pm(x, y, z^*) = 0 \quad (x, y) \in \Omega_d$$

$$\sigma_5^\pm(x, y, z^*) = 0$$

in which the superscripts + and - refer to the quantities related to the buckling layer and the sublaminates, respectively. For orthotropic shells, the conditions are equivalent to the requirement that the corresponding strains be zero on these surfaces. Therefore,

$$\varepsilon_4(x, y, \pm h/2) = 0 \quad (x, y) \in \Omega$$

$$\varepsilon_5(x, y, \pm h/2) = 0$$

$$\varepsilon_4^\pm(x, y, z^*) = 0 \quad (x, y) \in \Omega_d$$

$$\varepsilon_5^\pm(x, y, z^*) = 0$$

Applying these stress-free boundary conditions to Eq. (3) and using the displacement expression (1), one can identify some higher-order terms in terms of lower-order terms as follows, where  $i, k = 0, 1, 2, j = 1, 2, \dots, N - 2, m = N - 1, N$ , and  $\alpha = 1, 2$ :

$$U_{\alpha m}^{(i)}(x, y) = \psi_{\alpha m}^{(i)}[x, y; U_{\alpha j}^{(k)}, W^{(k)}] \quad (7)$$

Using the preceding expression, the refined displacement field, which satisfies all of the boundary conditions, can be defined as follows:

$$\begin{aligned}
 u_\alpha(x, y, z) &= \sum_{j=0}^{N-2} z^j U_{\alpha j}^{(0)}(x, y) \\
 &+ \sum_{j=N-1}^N z^j \psi_{\alpha j}^{(0)}(x, y) + [1 - H(z^*)] \\
 &\times \left[ \sum_{j=0}^{N-2} z^j U_{\alpha j}^{(1)}(x, y) + \sum_{j=N-1}^N z^j \psi_{\alpha j}^{(1)}(x, y) \right] \\
 &+ H(z^*) \left[ \sum_{j=0}^{N-2} z^j U_{\alpha j}^{(2)}(x, y) + \sum_{j=N-1}^N z^j \psi_{\alpha j}^{(2)}(x, y) \right] \\
 u_3(x, y, z) &= W^{(0)}(x, y) + [1 - H(z^*)]W^{(1)}(x, y) \\
 &+ H(z^*)W^{(2)}(x, y) \tag{8}
 \end{aligned}$$

In the present paper, up to fourth-order transverse shear correct terms ( $N = 4$ ) are used to formulate the displacement field. The specific form of the higher-order terms  $U_{\alpha m}^{(i)}$  is presented in the Appendix.

**B. Buckling and Postbuckling of Cylindrical Shells**

Consider a cylindrical shell that is subject to an in-plane compressive load distribution  $p$  at the midsurface in the direction normal to the boundary of the shell (Fig. 1). The minimum total potential energy principle is used to derive the governing equations and associated boundary conditions. For linear buckling analysis, the prebuckling state is assumed to be a membrane primary state since the axial compressive load is applied statically. This is characterized by

$$\sigma_i = \begin{cases} p, & i = 1 \\ 0, & i = 2, 4, 5, 6 \end{cases} \tag{9}$$

The second-order work done by the prebuckling stress can be expressed as follows:

$$\delta W = \int_{\Omega} p h u_{3,x} \delta u_{3,x} d\Gamma \tag{10}$$

where  $W$  is the work done by the applied compressive loads. The variational principle of the total potential energy is given by

$$\delta \Pi = \int_{\Omega} \int_{-h/2}^{h/2} \sigma_i \delta \varepsilon_i dz d\Omega - \int_{\Omega} p h u_{3,x} \delta u_{3,x} d\Gamma = 0 \tag{11}$$

Following Eqs. (1–4), the strains and stresses can also be written in the following form:

$$\begin{aligned}
 \varepsilon_i &= \varepsilon_i^{(0)} + [1 - H(z^*)]\varepsilon_i^{(1)} + H(z^*)\varepsilon_i^{(2)} \\
 \sigma_i &= \sigma_i^{(0)} + [1 - H(z^*)]\sigma_i^{(1)} + H(z^*)\sigma_i^{(2)} \tag{12}
 \end{aligned}$$

Equation (11) can now be rewritten based on two integral regions, the nondelamination region  $\Omega - \Omega_d$  and the delamination region  $\Omega_d$ , as follows:

$$\begin{aligned}
 &\int_{\Omega - \Omega_d} \left[ \int_{-h/2}^{h/2} \sigma_i^{(0)} \delta \varepsilon_i^{(0)} dz - p h W_{,x}^{(0)} \delta W_{,x}^{(0)} \right] d\Omega \\
 &+ \int_{\Omega_d} \left( \int_{-h/2}^{z^*} \{ [\sigma_i^{(i)} + \sigma_i^{(0)}] \delta \varepsilon_i^{(i)} + \sigma_i^{(i)} \delta \varepsilon_i^{(0)} \} dz \right. \\
 &- p \left( \frac{h}{2} + z^* \right) \{ [W_{,x}^{(1)} + W_{,x}^{(0)}] \delta W_{,x}^{(1)} + W_{,x}^{(1)} \delta W_{,x}^{(0)} \} \\
 &+ \int_{\Omega_d} \left( \int_{z^*}^{h/2} \{ [\sigma_i^{(2)} + \sigma_i^{(0)}] \delta \varepsilon_i^{(2)} + \sigma_i^{(2)} \delta \varepsilon_i^{(0)} \} dz \right. \\
 &- p \left( \frac{h}{2} - z^* \right) \{ [W_{,x}^{(2)} + W_{,x}^{(0)}] \delta W_{,x}^{(2)} + W_{,x}^{(2)} \delta W_{,x}^{(0)} \} \Big) d\Omega = 0 \tag{13}
 \end{aligned}$$

Integration of Eq. (13), through the thickness, yields the following equation:

$$\begin{aligned}
 &\int_{\Omega - \Omega_d} \left\{ N_{1j}^{(0)} \delta U_{1j,x}^{(0)} + N_{2j}^{(0)} \delta U_{2j,y}^{(0)} + N_{6j}^{(0)} \delta [U_{1j,y}^{(0)} + U_{2j,x}^{(0)}] \right. \\
 &+ N_{5j}^{(0)} \delta [(j+1)U_{1(j+1)}^{(0)} + W_{,x}^{(0)}] + N_{4j}^{(0)} \delta [(j+1)U_{2(j+1)}^{(0)} \\
 &+ W_{,y}^{(0)} - \frac{U_{2j}^{(0)}}{R}] - p h W_{,x}^{(0)} \delta W_{,x}^{(0)} \Big\} d\Omega \\
 &+ \int_{\Omega_d} \left( [N_{1j}^{(1)} + N_{1j}^{(10)}] \delta U_{1j,x}^{(1)} + N_{1j}^{(1)} \delta U_{1j,x}^{(0)} + [N_{2j}^{(1)} + N_{2j}^{(10)}] \right. \\
 &\times \delta U_{2j,y}^{(0)} + N_{2j}^{(1)} \delta U_{2j,y}^{(0)} + [N_{6j}^{(1)} + N_{6j}^{(10)}] \delta [U_{1j,y}^{(1)} + U_{2j,x}^{(1)}] \\
 &+ N_{6j}^{(1)} \delta [U_{1j,y}^{(0)} + U_{2j,x}^{(0)}] + [N_{5j}^{(1)} + N_{5j}^{(10)}] \\
 &\times \delta [(j+1)U_{1(j+1)}^{(1)} + W_{,x}^{(1)}] + N_{5j}^{(1)} \delta [(j+1)U_{1(j+1)}^{(0)} + W_{,x}^{(0)}] \\
 &+ [N_{4j}^{(1)} + N_{4j}^{(10)}] \delta \left[ (j+1)U_{2(j+1)}^{(1)} + W_{,y}^{(1)} - \frac{U_{2j}^{(1)}}{R} \right] \\
 &+ N_{4j}^{(10)} \delta \left[ (j+1)U_{2(j+1)}^{(0)} + W_{,y}^{(0)} - \frac{U_{2j}^{(0)}}{R} \right] - p \left( \frac{h}{2} + z^* \right) \\
 &\times \{ [W_{,x}^{(1)} + W_{,x}^{(0)}] \delta W_{,x}^{(1)} + W_{,x}^{(1)} \delta W_{,x}^{(0)} \} + [N_{1j}^{(2)} + N_{1j}^{(20)}] \\
 &\times \delta U_{1j,x}^{(2)} + N_{1j}^{(2)} \delta U_{1j,x}^{(0)} + [N_{2j}^{(2)} + N_{2j}^{(20)}] \delta U_{2j,y}^{(0)} \\
 &+ N_{2j}^{(2)} \delta U_{2j,y}^{(0)} + [N_{6j}^{(2)} + N_{6j}^{(20)}] \times \delta [U_{1j,y}^{(2)} + U_{2j,x}^{(2)}] \\
 &+ N_{6j}^{(2)} \delta [U_{1j,y}^{(0)} + U_{2j,x}^{(0)}] + [N_{5j}^{(2)} + N_{5j}^{(20)}] \\
 &\times \delta [(j+1)U_{1(j+1)}^{(2)} + W_{,x}^{(2)}] + N_{5j}^{(2)} \delta [(j+1)U_{1(j+1)}^{(0)} + W_{,x}^{(0)}] \\
 &+ [N_{4j}^{(2)} + N_{4j}^{(20)}] \delta \left[ (j+1)U_{2(j+1)}^{(2)} + W_{,y}^{(2)} - \frac{U_{2j}^{(2)}}{R} \right] \\
 &+ N_{4j}^{(20)} \delta \left[ (j+1)U_{2(j+1)}^{(0)} + W_{,y}^{(0)} - \frac{U_{2j}^{(0)}}{R} \right] - p \left( \frac{h}{2} - z^* \right) \\
 &\times \{ [W_{,x}^{(2)} + W_{,x}^{(0)}] \delta W_{,x}^{(2)} + W_{,x}^{(2)} \delta W_{,x}^{(0)} \} \Big) d\Omega = 0 \tag{14}
 \end{aligned}$$

where the stress resultants are defined as

$$\begin{aligned}
 N_{ij}^{(0)} &= \int_{-h/2}^{h/2} \sigma_i^{(0)} z^{j-1} dz \\
 N_{ij}^{(1)} &= \int_{-h/2}^{z^*} \sigma_i^{(1)} z^{j-1} dz, \quad N_{ij}^{(10)} = \int_{-h/2}^{z^*} \sigma_i^{(0)} z^{j-1} dz \tag{15} \\
 N_{ij}^{(2)} &= \int_{z^*}^{h/2} \sigma_i^{(2)} z^{j-1} dz, \quad N_{ij}^{20} = \int_{z^*}^{h/2} \sigma_i^{(0)} z^{j-1} dz
 \end{aligned}$$

Using Eqs. (1–4), the stress resultants in Eq. (15) can be expressed in terms of the generalized displacements. Furthermore, replacing the higher-order terms  $U_{\alpha N}^{(i)}$  and  $U_{\alpha(N-1)}^{(i)}$  ( $i = 0, 1, 2$  and  $\alpha = 1, 2$ ) with the expressions that are identified by solving Eq. (7), one can write the final form of Eq. (14) in terms of the generalized displacement variables,  $U_{\alpha j}^{(i)}$  ( $j = 0, 1, 2, \dots, N-2$ ) and  $W^{(i)}$ . By collecting terms involving the variations of functions  $U_{\alpha j}^{(i)}$  and  $W^{(i)}$  separately, a total of  $3(2N - 1)$  governing equations are obtained that are not presented here because of length restrictions.

For the nonlinear postbuckling analysis, the principle of minimum potential energy is written based on two integral regions, the nondelamination region  $\Omega - \Omega_d$  and the delamination region  $\Omega_d$ , as follows:

$$\begin{aligned} \delta \Pi = & \int_{\Omega - \Omega_d} \int_{-h/2}^{h/2} \sigma_{ij}^{(0)} \delta \varepsilon_{ij}^{(0)} dz d\Omega \\ & + \int_{\Omega_d} \left( \int_{-h/2}^{z^*} \{ [\sigma_{ij}^{(1)} + \sigma_{ij}^{(0)}] \delta \varepsilon_{ij}^{(1)} + \sigma_{ij}^{(1)} \delta \varepsilon_{ij}^{(0)} \} dz \right. \\ & \left. + \int_{z^*}^{h/2} \{ [\sigma_{ij}^{(2)} + \sigma_{ij}^{(0)}] \delta \varepsilon_{ij}^{(2)} + \sigma_{ij}^{(2)} \delta \varepsilon_{ij}^{(0)} \} dz \right) d\Omega \\ & - \int_{\Gamma_\sigma} p h \delta u_1 d\Gamma = 0 \end{aligned} \quad (16)$$

The superscript  $i$  denotes the stress and strain components corresponding to the variables  $U_{\alpha j}^{(i)}$  and  $W^{(i)}$  in the displacement expression [Eq. (1)]. Combining Eq. (16) with the nonlinear Mushtari–Vlasov–Donnell strain-displacement relations, Eq. (3), and the layer constitutive equation, Eq. (4), one can express the equilibrium equation in terms of the displacements as follows:

$$L_k [U_{\alpha j}^{(i)}, W^{(i)}] + N_k [U_{\alpha j}^{(i)}, W^{(i)}] = 0 \quad k = 1, 2, \dots, 3(2N + 1) \quad (17)$$

The associated boundary conditions are

$$B_{k^*} [U_{\alpha j}^{(i)}, W^{(i)}] = \eta_{k^*} \quad k^* = 1, 2, \dots, 3(2N + 2) \quad (18)$$

A separated solution is employed in the form of a double infinite trigonometric series (see Ref. 16), and the Rayleigh–Ritz method is used to obtain the nonlinear set of algebraic equations. In general, the following matrix form is used to express the nonlinear governing equations:

$$(\mathbf{K}_L + \mathbf{K}_N) \mathbf{a} = \mathbf{f} \quad (19)$$

where  $\mathbf{f}$  is the load vector. The nonlinear equations are solved using the Riks–Wempner incremental iterative scheme<sup>18–20</sup> to follow the pre- and postbuckling paths even through the limit point. In matrix notation, the buckling equations can be expressed as follows:

$$(\mathbf{K}_L + \lambda \mathbf{K}_G) \mathbf{a} = 0 \quad (20)$$

This eigenvalue problem associated with bifurcation (buckling) analysis is solved to obtain the critical load of the composite cylindrical shell with delamination.

In postbuckling analysis, a linearized buckling analysis is performed before the full nonlinear analysis to select those modes that dominate the prebuckling and buckling behavior of the composite shell.<sup>13,14</sup> Numerical tests show that the criterion can be profitably used to select the modes to be included in the displacement expansion, thus greatly reducing the required core size and the time required for obtaining the numerical solution.<sup>14</sup> In the following examples, 12 terms (or modes) in the double trigonometric series are selected, in each case, to ensure numerical precision. Under the no contact assumption, no normal surface traction is considered at delaminated surfaces during and after buckling regardless of whether or not the buckling modes imply contact. Since the contact during and after buckling may tend to increase the load-carrying capacity, the current study presents the results under the more critical condition.

### III. Results and Discussions

An example of a cylindrical shell made of isotropic material with clamped ends ( $u = v = w = w_x = 0$ ) under axial compression is presented to validate the proposed theory. The delamination lies at  $0.3h$  from the outer surface and it spans the entire circumference (Fig. 1). The dimensions of the shell are such that  $L/R = 5$  and  $R/h = 30$ . Each lamina of the shell is assumed to be isotropic. The numerical results of variation of critical load with delamination

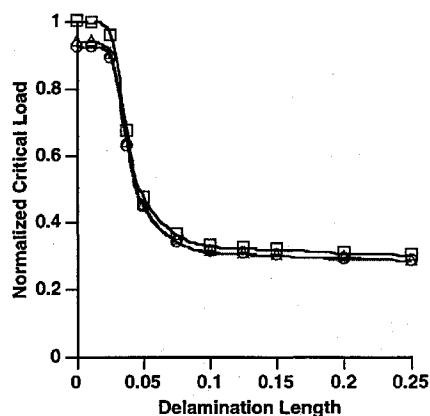


Fig. 2 Effect of transverse shear on critical load for the isotropic shell (validation example):  $\square$ , classical laminate theory;  $\triangle$ , first-order theory; and  $\circ$ , present theory.

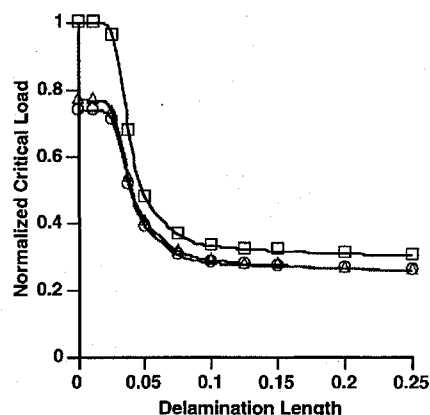


Fig. 3 Effect of transverse shear on critical load for cross-ply composite shells,  $R/h = 30$ :  $\square$ , classical laminate theory;  $\triangle$ , first-order theory; and  $\circ$ , present theory.

length, obtained using the present theory, are compared with those obtained using existing solutions as shown in Fig. 2. The square data points indicate the solutions presented in Ref. 9, in which the transverse shear effects are not included. It is shown that the critical load computed from the classical laminate theory deviates substantially from those derived using the proposed theory. In the example, where the radius-to-thickness ratio is considerably large ( $R/h = 30$ ) and the material is isotropic, a case for which the classical laminate theory is generally regarded to be accurate for plate, a deviation of about 7.5% is observed in the value of the critical load. This indicates that the transverse shear effect plays a very significant role in cylindrical shells. The effects are even larger than those observed in composite plates.<sup>15</sup> This observation agrees with that reported by Kardomateas,<sup>21</sup> which is that for isotropic cylindrical shells the refined theory predicts a much lower critical load than the simplified Donnell shell theory.

The linear buckling analyses are performed with shells made of frequently used composites. The shell is subjected to an uniform in-plane axial compressive load. Examples are presented for cross-ply laminates with a stacking sequence of  $[0/90/0]_{10}$  and angle-ply laminates with a stacking sequence of  $[-45/45]_{8S}$ . Both ends are assumed to be clamped. The material used is graphite/epoxy with the following engineering constants:

$$\begin{aligned} E_L/E_T &= 40, & G_{LT}/E_T &= 0.5 \\ G_{TT}/G_{LT} &= 1.0 & \nu_{LT} &= 0.25 \end{aligned}$$

Comparisons of the transverse shear effect on the normalized critical load, with changes in the magnitude of the delamination length parameter  $\beta$ , are presented in Fig. 3 for the  $[0/90/0]_{10}$  shell and in Fig. 4 for the  $[-45/45]_{8S}$  shell. The delamination is positioned

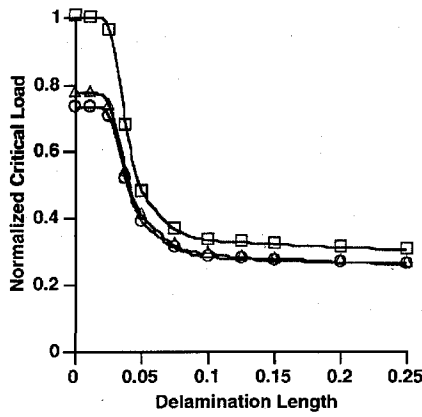


Fig. 4 Effect of transverse shear on critical load for the angle-ply composite shell,  $R/h = 30$ :  $\square$ , classical laminate theory;  $\triangle$ , first-order theory; and  $\circ$ , present theory.

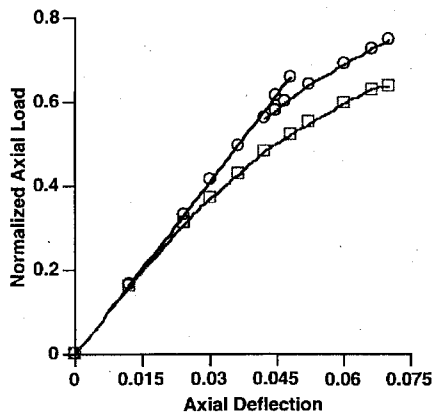


Fig. 5 Variation of normalized load with axial deflection during postbuckling for the composite shell:  $\circ$ ,  $\beta = 0.005$  and  $\square$ ,  $\beta = 0.035$ .

symmetrically in the axial direction. It is seen that transverse shear effect becomes smaller as the delamination length increases. This is because, with the increase in the delamination length, local buckling of the delaminated layer becomes dominant, which causes the local radius-to-thickness ratio to be larger. Therefore the transverse shear effect decreases. Slightly larger transverse shear effect is seen in Fig. 4 for the  $[-45/45]_{8S}$  shell than for the  $[0/90/0]_{10}$  shell in Fig. 3. Larger deviations between the first-order theory and the present theory are also observed in the case of the angle ply, over a wide range of  $R/h$  values, in Fig. 4 than in Fig. 3 for the cross ply. Finally, more significant deviations between the first-order theory and the present theory are observed in cases of composite shells than in isotropic shells.

The results of the postbuckling analysis is presented in Fig. 5, which shows the variation of the axial load with the axial deflection for two different size of initial delamination,  $\beta = 0.005$  and  $0.035$ . The delamination lies at the same position ( $0.3h$ ) as in the preceding example. The shell considered here is moderately thick,  $h = 2.54$  cm, with dimensions  $R = 91.4$  cm and  $L = 254$  cm. The axial load is normalized with respect to the critical load obtained from linear buckling analysis for the same shell without delamination. The maximum load for the short delamination case is approximately two-thirds of the critical load predicted by the linear analysis, whereas the minimum postbuckling load is about 0.6 times the critical load. According to Pedersen,<sup>22,23</sup> the maximum load can be reached only for shells with very small imperfections. As shown here, the maximum load can be reached only for shells with very short delaminations. For longer delaminations, a gradual transition from the pure membrane prebuckling behavior to the postbuckling response occurs.

The equilibrium path for the cross-ply composite shell with a stacking sequence of  $[0/90/0]_{10}$  and the angle-ply composite shell

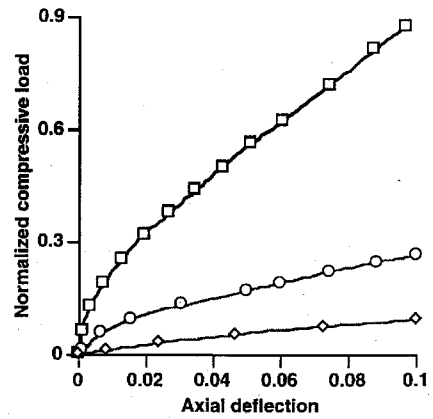


Fig. 6 Variation of normalized load with axial deflection during postbuckling for cross-ply composite shells:  $\square$ ,  $\beta = 0.01$ ;  $\circ$ ,  $\beta = 0.06$ ; and  $\diamond$ ,  $\beta = 0.095$ .

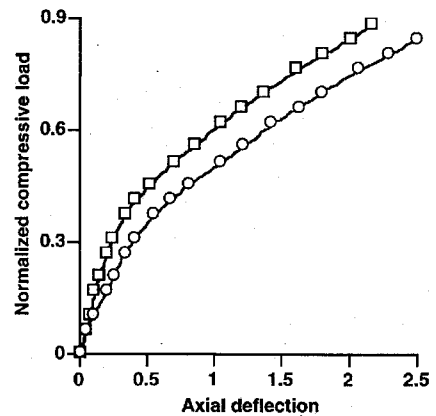


Fig. 7 Variation of normalized load with axial deflection during postbuckling for angle-ply composite shells:  $\square$ ,  $\beta = 0.01$  and  $\circ$ ,  $\beta = 0.05$ .

with a stacking sequence of  $[-45/45]_{8S}$  are plotted in Figs. 6 and 7, where the compressive loads are normalized with respect to the critical load for the shell without delamination and the axial deflections are normalized with respect to the thickness  $h$ . The dimensions of the shell considered here are  $L/R = 5$  and  $R/h = 30$ . It is seen that as delamination length increases, the load capacity drops sharply in both cases of cross-ply and angle ply shells. In the cross-ply case, the load-carrying capacity of the shell with delamination parameter  $\beta = 0.95$  is only about one-ninth of the shell with  $\beta = 0.01$ . The axial deflections (end shortening) for the angle-ply shell are much larger than those for the cross-ply shell because of the weakness in axial stiffness of the angle-ply shell. The trends displayed by these load-displacement curves are similar to those presented by Yin<sup>24</sup> for delaminated laminates. This implies the general agreement between the postbuckling behavior of delaminated thick composite cylindrical shells and delaminated flat laminates.

Figures 8–10 illustrate the variations of the midpoint deflections, normalized by the shell thickness  $h$  over a wide range of normalized compressive loads for delaminated layers and bottom sublaminates. Both cross-ply and angle-ply cases are considered. For the short delamination length (Fig. 8), the delaminated layer and the bottom sublaminates are not separated even as the load increases. This means that the shell fails at the global mode. However, for the larger delamination length (Fig. 9), the deflections of the delaminated layer increase rapidly, whereas the deflections for the bottom sublaminates are stable after reaching a certain value. In this case, it is clear that the shell failure is governed by a local mode. Similar trends are observed for the angle-ply case in Fig. 10. These observations also agree with the discussions regarding the mode shapes in delamination buckling of composite plates presented in Refs. 15 and 25.

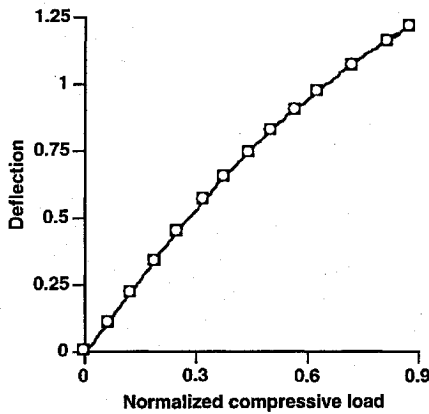


Fig. 8 Midpoint deflection of delaminated layer and sublaminates for cross-ply shells,  $\beta = 0.01$ :  $\square$ , bottom layer and  $\circ$ , delaminated layer.

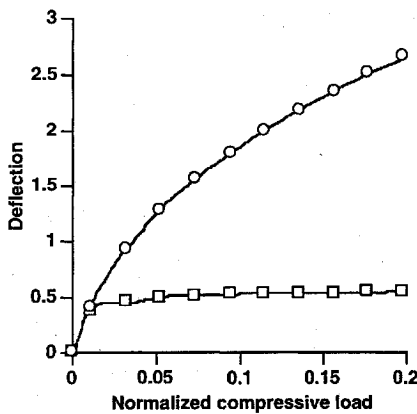


Fig. 9 Midpoint deflection of delaminated layer and sublaminates for cross-ply shells,  $\beta = 0.095$ :  $\square$ , bottom layer and  $\circ$ , delaminated layer.

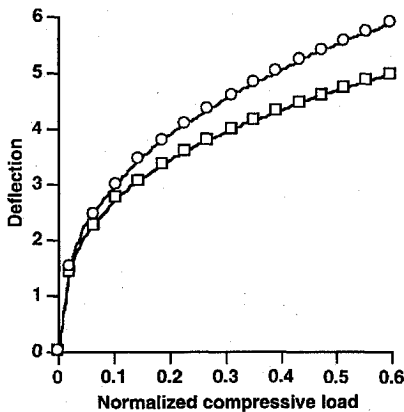


Fig. 10 Midpoint deflection of delaminated layer and sublaminates for angle-ply shells,  $\beta = 0.05$ :  $\square$ , bottom layer and  $\circ$ , delaminated layer.

#### IV. Concluding Remarks

A new higher-order theory is developed to study the delamination buckling and postbuckling problem in composite cylindrical shells. The refined displacement field proposed in this paper is capable of representing displacement discontinuity conditions at the interface of the existing delamination as well as in satisfying the transverse shear stress-free conditions at surfaces and at the delamination interface. Numerical investigations of the transverse shear effect on critical buckling load and nonlinear postbuckling equilibrium path are performed. The following important observations are made from this study.

- 1) The present theory provides an adequate framework for the analysis of composite cylindrical shells with delaminations. Particularly, the theory is expected to obtain accurate displacement distributions with lower computational cost for engineering applications.
- 2) For laminated composite shells, the transverse shear effect on delamination buckling is very significant.
- 3) The maximum load can be reached only for shells with very short delaminations. A gradual transition from the pure membrane prebuckling behavior to the postbuckling response occurs for longer delaminations.
- 4) Since delamination is a type of imperfection, even a small size of the initial delamination reduces the load capacity very sharply.
- 5) Delamination plays an important role in the buckling and postbuckling modes, thereby governing the cylindrical shell failure mechanism.

#### Appendix: Identification of Higher-Order Terms

The expression of identified higher-order terms solved in Eq. (7) are given here for special case of  $N = 4$ :

$$U_{13}^{(0)} = -(4/3h^2)[U_{11}^{(0)} + W_{,x}^{(0)}] \quad U_{14}^{(0)} = -(2/h^2)U_{12}^{(0)}$$

$$U_{23}^{(0)} = -\frac{1}{(48R^2 - h^2)h^2} \{64R[RW_{,y}^{(0)} - U_{20}^{(0)}] + 4(16R^2 - h^2)U_{21}^{(0)} - 8R^2U_{22}^{(0)}\}$$

$$U_{24}^{(0)} = -\frac{1}{(48R^2 - h^2)h^2} \{16[RW_{,y}^{(0)} - U_{20}^{(0)}] - 32RU_{22}^{(0)} + 4(24R^2 - h^2)U_{22}^{(0)}\}$$

$$U_{13}^{(1)} = -\frac{4}{3h^2\alpha^2} \{(1 - \alpha)[U_{11}^{(1)} + W_{,x}^{(0)}] + h\alpha(1 - \alpha) \times [U_{12}^{(1)} + U_{12}^{(0)}] + (1 - \alpha + \alpha^2)[U_{11}^{(1)} + W_{,x}^{(1)}]\}$$

$$U_{14}^{(1)} = -\frac{2(1 - \alpha)}{h^3\alpha^2} \left\{ U_{11}^{(1)} + W_{,x}^{(0)} + h\alpha \left[ \frac{U_{12}^{(1)}}{1 - \alpha} + U_{12}^{(0)} \right] + U_{11}^{(1)} + W_{,x}^{(1)} \right\}$$

$$U_{23}^{(1)} = -\frac{2}{a_{11}} \left( 2[(8R - h\alpha)(2R + h) + \alpha^3(8R + h) \times (2R - h\alpha)]U_{21}^{(1)} + h\alpha[(8R + h) \times (4R - h\alpha) - \alpha^2(8R - h\alpha)(4R + h)]U_{22}^{(1)} + 4[8R + h + \alpha^3(8R - h\alpha)][RW_{,y}^{(1)} - U_{20}^{(1)}] + 2(8R + h) \times \left\{ 2R - h\alpha - \frac{\alpha^2}{(48R^2 - h^2)}[(16R^2 - h^2) \right. \right.$$

$$\left. \times (6R - h\alpha) - 4Rh\alpha(8R - h\alpha) \right\} U_{21}^{(0)} + h\alpha(8R + h)$$

$$\times \left\{ 4R - h\alpha + \frac{\alpha}{(48R^2 - h^2)}[4Rh(6R - h\alpha) \right.$$

$$\left. - \alpha^2(24R^2 - h^2)(8R - h\alpha) \right\} U_{22}^{(0)} + 4(8R + h)$$

$$\times \left\{ 1 - \frac{\alpha^2}{(48R^2 - h^2)}[8R(6R - h\alpha) \right.$$

$$\left. + h\alpha(8R - h\alpha) \right\} [RW_{,y}^{(0)} - U_{20}^{(0)}]$$

$$\begin{aligned}
 U_{24}^{(1)} = & -\frac{4}{a_{12}} \left( 2[(6R+h)(2R-h\alpha) - \alpha^2(6R-h\alpha)] \right. \\
 & \times (2R+h)U_{21}^{(1)} + h\alpha[(6R+h)(4R-h\alpha) - \alpha(6R-h\alpha)] \\
 & + \alpha(6R-h\alpha)(4R+h)U_{22}^{(1)} + 4[6R+h - \alpha^2(6R-h\alpha)] \\
 & \times [RW_{,y}^{(1)} - U_{20}^{(1)}] + 2(6R+h) \\
 & \times \left\{ 2R-h\alpha - \frac{\alpha^2}{(48R^2-h^2)} [(16R^2-h^2)] \right. \\
 & \times (6R-h\alpha) - 4Rh\alpha(8R-h\alpha) \left. \right\} U_{21}^{(0)} + h\alpha(6R+h) \\
 & \times \left\{ 4R-h\alpha + \frac{\alpha}{48R^2-h^2} [4Rh(6R-h\alpha) - \alpha(24R^2-h^2)] \right. \\
 & \times (8R-h\alpha) \left. \right\} U_{22}^{(0)} + 4(6R+h) \left\{ 1 - \frac{4\alpha^2}{(48R^2-h^2)} \right. \\
 & \times [8R(6R-h\alpha) - h\alpha(8R-h\alpha)] [RW_{,y}^{(0)} - U_{20}^{(0)}] \left. \right\} \\
 a_{11} = & h^2\alpha^2[(8R+h)(6R-h\alpha) + \alpha(8R-h\alpha)(6R+h)] \\
 a_{12} = & h^3\alpha^2[(8R+h)(6R-h\alpha) + \alpha(8R-h\alpha)(6R+h)]
 \end{aligned}
 \tag{A1a}$$

$$\begin{aligned}
 U_{13}^{(2)} = & -\frac{4}{3h^2\alpha^2} \{ (1+\alpha)[U_{11}^{(1)} + W_{,x}^{(0)}] \\
 & + h\alpha(1+\alpha)[U_{12}^{(1)} + U_{12}^{(0)}] + (1+\alpha+\alpha^2)[U_{11}^{(1)} + W_{,x}^{(1)}] \}
 \end{aligned}$$

$$U_{14}^{(2)} = \frac{2(1+\alpha)}{h^3\alpha^2} \left\{ U_{11}^{(1)} + W_{,x}^{(0)} + h\alpha \left[ \frac{U_{12}^{(1)}}{1+\alpha} + U_{12}^{(0)} \right] + U_{11}^{(1)} + W_{,x}^{(1)} \right\}$$

$$\begin{aligned}
 U_{23}^{(2)} = & -\frac{2}{a_{21}} \left( 2[(8R+h)(2R-h\alpha) - \alpha^3(8R-h\alpha)] \right. \\
 & \times (2R+h)U_{21}^{(1)} + h\alpha[(8R+h) \\
 & \times (4R-h\alpha) - \alpha^2(8R-h\alpha)(4R+h)]U_{22}^{(1)} \\
 & + 4[8R+h - \alpha^3(8R-h\alpha)] \\
 & \times [RW_{,y}^{(1)} - U_{20}^{(1)}] + 2(8R+h) \\
 & \times \left\{ 2R-h\alpha - \frac{\alpha^2}{(48R^2-h^2)} [(16R^2-h^2)] \right. \\
 & \times (6R-h\alpha) - 4Rh\alpha(8R-h\alpha) \left. \right\} U_{21}^{(0)} + h\alpha(8R+h) \\
 & \times \left\{ 4R-h\alpha - \frac{\alpha}{(48R^2-h^2)} [4Rh(6R-h\alpha) \right. \\
 & - \alpha^2(24R^2-h^2)(8R-h\alpha)] \left. \right\} U_{22}^{(0)} + 4(8R+h) \\
 & \times \left\{ 1 - \frac{\alpha^2}{(48R^2-h^2)} [8R(6R-h\alpha) \right. \\
 & + h\alpha(8R-h\alpha)] [RW_{,y}^{(0)} - U_{20}^{(0)}] \left. \right\}
 \end{aligned}$$

$$\begin{aligned}
 U_{24}^{(2)} = & \frac{4}{a_{22}} \left( 2[(6R+h)(2R-h\alpha) - \alpha^2(6R-h\alpha)] \right. \\
 & \times (2R+h)U_{21}^{(1)} + h\alpha[(6R+h)(4R-h\alpha) - \alpha(6R-h\alpha)] \\
 & \times (4R+h)U_{22}^{(1)} + 4[6R+h - \alpha^2(6R-h\alpha)] \\
 & \times [RW_{,y}^{(1)} - U_{20}^{(1)}] + 2(6R+h) \left\{ 2R-h\alpha - \frac{\alpha^2}{(48R^2-h^2)} \right. \\
 & \times [(16R^2-h^2)(6R-h\alpha) - 4Rh\alpha(8R-h\alpha)] \left. \right\} \\
 & \times U_{21}^{(0)} + h\alpha(6R+h) \left\{ 4R-h\alpha + \frac{\alpha}{(48R^2-h^2)} \right. \\
 & \times [4Rh(6R-h\alpha) - \alpha(24R^2-h^2)(8R-h\alpha)] \left. \right\} U_{22}^{(0)} \\
 & + 4(6R+h) \left\{ 1 - \frac{4\alpha^2}{(48R^2-h^2)} \right. \\
 & \times [8R(6R-h\alpha) - h\alpha(8R-h\alpha)] [RW_{,y}^{(0)} - U_{20}^{(0)}] \left. \right\} \\
 a_{21} = & h^2\alpha^2[(8R+h)(6R-h\alpha) - \alpha(8R-h\alpha)(6R+h)] \\
 a_{22} = & h^3\alpha^2[(8R+h)(6R-h\alpha) - \alpha(8R-h\alpha)(6R+h)]
 \end{aligned}$$

with

$$\alpha = 2z^*/h \tag{A1b}$$

**Acknowledgment**

The research was supported by U.S. Army Research Office Grant DAAH04-93-G-0043.

**References**

- <sup>1</sup>Chai, H., Babcock, C. D., and Krauss, W. G., "One Dimensional Modeling of Failure in Delaminated Laminates," *International Journal of Solid and Structures*, Vol. 17, No. 11, 1981, pp. 1069-1083.
- <sup>2</sup>Chai, H., and Babcock, C. D., "Two-Dimensional Modeling of Failure in Laminated Plates by Delamination Buckling," *Journal of Composite Materials*, Vol. 19, Jan. 1985, pp. 67-98.
- <sup>3</sup>Sallam, S., and Simitse, G. J., "Delamination Buckling and Growth of Flat, Cross-ply Laminates," *Composite Structures*, Vol. 4, No. 4, 1985, pp. 361-381.
- <sup>4</sup>Kardomateas, G. A., and Schmueser, D. W., "Buckling and Postbuckling of Delaminated Composites Under Compressive Loads Including Transverse Shear Effects," *AIAA Journal*, Vol. 26, No. 3, 1988, pp. 337-343.
- <sup>5</sup>Barbero, E. J., and Reddy, J. N., "Modeling of Delamination in Composite Laminates Using a Layer-Wise Plate Theory," *International Journal of Solid and Structures*, Vol. 28, No. 3, 1991, pp. 373-388.
- <sup>6</sup>Kulkarni, S. V., and Frederick, D., "Buckling of Partially Debonded Layered Cylindrical Shell," *Proceedings of the AIAA/ASME/SAE 14th Structures, Structural Dynamics, and Materials Conference* (Williamsburg, VA), AIAA, New York, 1973, pp. 168-174.
- <sup>7</sup>Jones, R. M., "Buckling of Stiffened Two-Layered Shell of Revolution with a Circumferentially Cracked Unbonded Layer," *AIAA Journal*, Vol. 7, No. 8, 1969, pp. 1511-1517.
- <sup>8</sup>Troshin, V. P., "Effect of Longitudinal Delamination in a Laminar Cylindrical Shell on the Critical External Pressure," *Journal of Composite Materials*, Vol. 17, No. 5, 1983, pp. 563-567.
- <sup>9</sup>Sallam, S., and Simitse, G. J., "Delamination Buckling of Cylindrical Shells Under Axial Compression," *Composite Structures*, Vol. 7, No. 2, 1987, pp. 83-101.
- <sup>10</sup>Chen, Z. Q., and Simitse, G. J., "Delamination Buckling of Pressure-Loaded Cross-Ply Laminated Cylindrical Shells," *ZAMM*, Vol. 68, No. 10, 1988, pp. 491-502.
- <sup>11</sup>Chen, Z. Q., and Simitse, G. J., "On the Postbuckling Behavior of a Delaminated Thin Cylindrical Shells," *Composite Structures 5*, edited by I. H. Marshall, Elsevier, London, 1989, pp. 447-465.
- <sup>12</sup>Kardomateas, G. A., and Chung, C. B., "Thin Film Modeling of Delamination Buckling in Pressure Loaded Laminated Cylindrical Shells," *AIAA Journal*, Vol. 30, No. 8, 1992, pp. 2119-2123.

<sup>13</sup>Simitses, G. J., and Anastasiadis, J. S., "Shear Deformable Theories for Cylindrical Laminates—Equilibrium and Buckling with Applications," *AIAA Journal*, Vol. 30, No. 3, 1992, pp. 826–834.

<sup>14</sup>Reddy, J. N., and Savoia, M., "Layer-Wise Shell Theory for Postbuckling of Laminated Circular Cylindrical Shells," *AIAA Journal*, Vol. 30, No. 8, 1992, pp. 2148–2154.

<sup>15</sup>Chattopadhyay, A., and Gu, H., "New Higher Order Plate Theory in Modeling Delamination Buckling of Composite Laminates," *AIAA Journal*, Vol. 32, No. 8, 1994, 1709–1716.

<sup>16</sup>Chattopadhyay, A., and Gu, H., "Modeling of Delamination Buckling in Composite Cylindrical Shells Using a New Higher-Order Theory," *Composite Science and Technology*, Vol. 54, No. 2, 1995, pp. 223–232.

<sup>17</sup>Lo, K. H., Christensen, R. M., and Wu, E. M., "A Higher-Order Theory of Plate Deformation (Part 2: Laminate Plates)," *Journal of Applied Mechanics*, Vol. 44, Dec. 1977, pp. 669–676.

<sup>18</sup>Riks, E., "An Incremental Approach to the Solution of Snapping and Buckling Problems," *International Journal of Solids and Structures*, Vol. 15, No. 7, 1979, pp. 529–551.

<sup>19</sup>Wempner, G. A., "Discrete Approximations Related to Nonlinear Theories of Solids," *International Journal of Solids and Structures*, Vol. 7, No. 11,

1971, pp. 1581–1599.

<sup>20</sup>Crisfield, M. A., "A Fast Incremental/Iterative Solution Procedure That Handles 'Snap-through,'" *Computers and Structures*, Vol. 13, Nos. 1–3, 1981, pp. 55–62.

<sup>21</sup>Kardomateas, G. A., "Stability Loss in Thick Transversely Isotropic Cylindrical Shells Under Axial Compression," *Journal of Applied Mechanics*, Vol. 60, June 1993, pp. 506–513.

<sup>22</sup>Pedersen, P. T., "On the Collapse Load of Cylindrical Shells," *Buckling of Structures*, edited by B. Budiansky, Springer-Verlag, Berlin, 1974, pp. 27–39.

<sup>23</sup>Pedersen, P. T., "Buckling of Unstiffened and Stiffened Cylindrical Shells Under Axial Pressure," *International Journal of Solids and Structures*, Vol. 9, No. 5, 1973, pp. 671–691.

<sup>24</sup>Yin, W.-L., "Cylindrical Buckling of Laminated and Delaminated Plates," *Proceedings of the AIAA 27th Structures, Structural Dynamics, and Materials Conference (Part 1)*, AIAA, Washington, DC, 1986, pp. 165–179.

<sup>25</sup>Yin, W., Sallam, S., and Simitses, G. J., "Ultimate Axial Load Capacity of a Delaminated Beam-Plate," *AIAA Journal*, Vol. 24, No. 1, 1986, pp. 123–128.